

**Violeta Gjeshovska**

PhD, Associate Professor  
University "Ss. Cyril and Methodius"  
Faculty of Civil Engineering - Skopje,  
N. Macedonia  
violetag@gf.ukim.edu.mk

**Bojan Ilioski**

MSc, Civil engineer  
University "Ss. Cyril and Methodius"  
Faculty of Civil Engineering - Skopje,  
N. Macedonia  
bojaniloski@hotmail.com

## **APPLICATION OF HEC-RAS FOR ANALYSIS OF FLOOD ZONES**

Timely forecasting of floods and floodplains allows measures to be taken to prevent or reduce their occurrence and/or to provide protection against their harmful effects. The flood wave from increase of the water level and the flow in the riverbed is defined as a non-stationary flow, which results in flooding of riverbeds. The use of hydraulic models to conduct flood simulations is a common practice and widely accepted for rapid and accurate definition of flood zones.

In the investigations presented in this paper, the HEC-RAS (1D, 2D, 1D / 2D) software package has been used to simulate different flood scenarios related to Vardar River.

Using the HEC-RAS software package, 1D, 2D and a combination of 1D and 2D models of a non-stationary flow have been formulated by defining the initial and the boundary conditions separately for each model. As a result of the simulation of the flood wave propagation through the riverbed, the flood zones and the most endangered areas have been defined. The obtained results and the differences among the considered models have been analyzed in order to see which model is the most appropriate for the case of a flood wave.

From the hydraulic analyses carried out by use of all three models, it is concluded that the riverbed of the Vardar river in the considered section has a very low transportation capacity and that there are flood zones along the entire length of the river. The riverbed of the Vardar river in the analyzed region, from the village Tudence to the village Jegunovce, can safely transform flows up to  $Q=62 \text{ m}^3/\text{s}$ .

**Keywords:** flood, flood wave, flood zones, HEC-RAS.

### **1. INTRODUCTION**

Floods are among the most devastating natural disasters affecting people and infrastructure. It is therefore not surprising that modeling and predicting such events is becoming a high priority in many countries, [1]. Flood modeling involves simulation of the processes of transformation of precipitation in the hydrograph of a flood wave and its propagation through the catchment area or the river bed, [2].

In this way, flood processes consisting of upstream systems with hydrological processes and river and flood zones with hydraulic processes - are described physically or mathematically (through the use of appropriate mathematical equations) by presentation of relationships between the state of the system, the input and the output.

To analyze the morphology of the Tigris River in Baghdad and determine the capability of the riverbed, A. A. Ali et al (2012) analyzed a section with a length of 49 km, with transverse profiles at intervals of 250 meters, [3]. For this purpose, they developed a one-dimensional hydraulic model with the help of the HEC-RAS software and calibrated the obtained results according to a 10-year analysis of data from the measuring station in Baghdad, whereat they concluded that the one-dimensional model is a good method for predicting the bandwidth of a riverbed. The hydraulic model developed by use of the HEC-RAS software proved to be a good way of modeling a flood wave that provides fast and accurate data. Santillan J.R. and Dr. Paringit E.C (2013) analyzed the floods from the Marikina River in the Philippines that occurred as a result of the heavy rainfall in the river basin, [4]. Hong Quang Nguyen (2015) used the HEC-RAS software bundled with KINEROS2 software for the floods in the tropical regions of northern Vietnam, [5]. With the final results of the research, he came to the conclusion that the HEC-RAS software works well with other software.

Thaileng Thol et al. (2016) presented an analysis of flood zones for the Mekong River in Cambodia using HEC-RAS, [6]. The results of the analysis with the model from HEC-RAS were compared with the measured data for that section of the river and these agreed with each other. The authors believe that HEC-RAS analyzes are a good way of timely predicting flood zones.

With the analysis for modeling and forecasting of flood zones, Vassiliki Terezinha Galvao Boulomytis (2017) came to the conclusion that poorly performed hydrological analysis is one of the biggest reasons for poor modeling of flood wave transformation, [7]. Romali, N. et al. (2018) applied the HEC-RAS model in flood mapping and simulation of a flood map for different return periods for an urban area in the town of Segamat in Malaysia, [8]. To calculate the extreme flows with different return periods, five distribution models were tested during the flood frequency analysis. The results showed that most of the flooded areas in the simulated 100-year return period were also affected by

the historic 2011 floods. Khalfallah and Saidi (2018) presented spatial-temporal mapping and flood forecasting by using HEC-RAS-GIS for the Meyerda River, Tunisia, [9]. The authors found that obtaining information about floods in regions with poor data is a difficult and uncertain task, but it is very valuable for flood risk management in order to protect human civilization and the environment. In order to find an effective model for analyzing flood wave transformation and perform flood zone analysis, Lea Dasallas et al. (2019) developed a combined one-dimensional and two-dimensional model for the 2011 Baeksan River flood case in South Korea. The results obtained from the model show great similarities with the measured data and data from different methods of analysis, which proves that the HEC-RAS software is an excellent method for analysis of this issue, [10]. Diedhiou, R. et al. (2020) performed hydraulic modeling of the Senegal River Basin downstream the Diamond Dam using the HEC-RAS software, [11]. The results obtained by the HEC-RAS simulations refer to variations of water level, maximum flow velocities and flood propagation time. These results suggest that HEC-RAS is a useful tool for making quick and timely flood management decisions in times of crisis.

Huțanu, E. et al. (2020) developed a one-dimensional model for analysis of flood zones for the Jijia River in Romania using HEC-RAS in order to compare the results of the model with those of the model already developed in the MIKE SHE software. The comparison of the models by the authors led to the conclusion that the model based on HEC-RAS gave better results and that the software itself provided a better display of the final results, [12].

Presented in this paper is a description of the development, calibration and validation of the flood model for the Vardar river basin (R. North Macedonia) by the widely used hydraulic modeling systems HEC-RAS, [13]. Hydraulic models 1D, 2D and a combination of 1D and 2D models of a non-stationary flow have been formulated by defining the initial and boundary conditions separately for each model. The differences between these models in terms of defining flood zones as well as the advantages of applying HEC-RAS in solving such problems are discussed.

## 2. STUDY AREA

The river Vardar is the largest river in the R.N. Macedonia. It is 388 km long, of which 301 km are located in the Republic of Macedonia. Its

basin covers approximately 25,000 km<sup>2</sup>, with a river basin area of 20,535 km<sup>2</sup> in the Macedonia. In this paper, the watershed of upper Vardar is analyzed, which extends upstream from the village of Radusa in the northwestern part of RN Macedonia, Figure 1. The catchment area of the river Vardar, opposite the village of Radusa, covers an area of 1489.19 km<sup>2</sup>. In height, the catchment area extends from elevation 2747.03 m above sea level to elevation 317.57 m asl. The terrain topography data around the Vardar River used in this analysis are in digital form (DTM-Digital Terrain Model). Using the SWAT model of the Geographic Information System (GIS) for spatial analysis (SA), [14], the watershed is drawn and the shape and size of the catchment area of the river Vardar to the village Radusa is determined, Figure 2. Characteristics of the watershed upstream of the village Radusa and the village of Jegunovce are shown in Table 1.



Figure 1. Location of the upper Vardar watershed



Figure 2. Form and size of upper Vardar watershed

Table 1. Geometrical characteristics of the upper Vardar watershed

Profile	A [km <sup>2</sup> ]	O [km]	Ssr [%]	Hsr [m asl]	L [km]
Radusa	1489.1	232.2	9.37	1138.8	101.4
Jegunov	1336.6	217.3	9.24	1152.8	94.55

## 2.1 LAND USE

For the needs of hydrological modeling of the Vardar river basin in the upper course to the village Radusa, analysis of land use and the representation of certain classes, was done accordance with the data from CORINE Layer Classification, [15]. The data are processed and interpreted by means of the GIS software moduli, Figure 3. Table 2 shows the land use of the basin of Goren Vardar to the village Radusa according to the CORINE classification.

The most present within the watershed, accounting for more than 1031 km<sup>2</sup> (69.3%), are forests and semi-natural areas. Out of these, forests account for 516 km<sup>2</sup> (34.51%). Dominant forests are the broadleaved ones, with minor presence of mixed forests and very little, almost negligible presence of coniferous forests. Coppice forests and grass vegetation is present both in the transition areas and the higher parts of the watershed. The most present in this group is natural grass accounting for 292.87km<sup>2</sup> (19.7%) of the total watershed area, then the coppice bush vegetation covering about 148.1 km<sup>2</sup>. Within the total area covered by coppice and grass vegetation amounting to 503.29 km<sup>2</sup> (33.86% of the watershed), wastelands or sclerophyllous vegetation are present to a minor scope. This category also includes open areas with little or no vegetation, accounting for about 1% of the watershed. Agricultural areas accounting for 408.0 km<sup>2</sup> (27.4%) are considerably present within the watershed and include arable land of 133.93 km<sup>2</sup>, some perennial plantations accounting for 4.48 km<sup>2</sup>, pastures accounting for 10.20 km<sup>2</sup>, and dominant 261.81km<sup>2</sup> (17.61%) of different agricultural areas (agricultural land and complex crop rotation lands). Within the watershed, artificial areas (urban areas, industrial, commercial and transportation structures, mines, landfills and construction sites) cover 49.5 km<sup>2</sup> (3.26%) of the total watershed area.

The scale of the used network (250x250 m) does not allow accurate definition of individual categories pertaining to the third level, for example, roads and railways that exist within

the watershed. This was probably the reason for not detecting marshes and swamps as well as water bodies (small lakes on Shar Mountain and along the water courses within the watershed). Hence, this analysis of presence of individual categories of land use should be considered only indicative and done for the purposes of hydrological analysis of the watershed.

Table 2. Geometrical characteristics of the upper Vardar watersheds

Category	Area $A [km^2]$
Artificial surfaces	49.5
Agricultural areas	409.0
Forests	1031.0
Wetlands	0.0
Water bodies	0.0
Total	1486.1

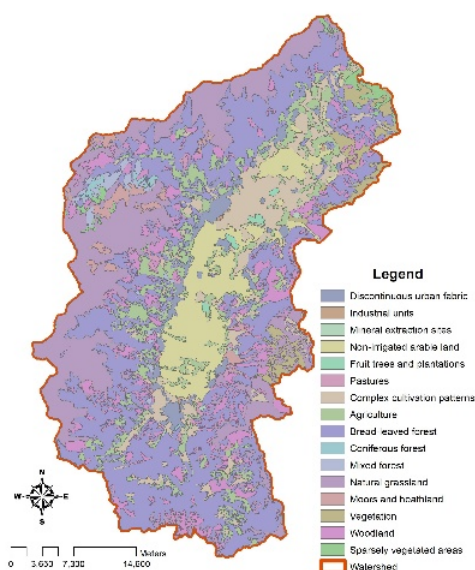


Figure 3. Land use classification

## 2.2 HYDROGRAPHIC CHARACTERISTICS

The river Vardar from the village Tudence to the village Jegunovce, in a total length of about 7 km, is located in the basin of Goren Vardar or in the lower part of the Polog valley. Dominant participation in the outflow and formation of flows in the river Vardar have surface waters coming from the northwestern massif, ie from the left tributaries of the river Vardar. These rivers come from the highlands of Shar Mountain, have a torrential character, carry a significant amount of sediment and flood and

degrade the fertile agricultural areas along the river Vardar. The Vardar river basin in this part is hydrographically more developed on the left side, where the larger tributaries are: Pena, Porojska / Dzepcishka, Bistrica and Vratnicka.

The length of the river Vardar to the profile in Radusa is 82.33 km, and the equivalent length of the watershed is 101.43 km. The maximum altitude in the watershed is 2746 m above sea level, while the minimum altitude curve of the Vardar river basin upstream of Radusa and the summary line of the altitude distribution are shown in Figure 4. Larger tributaries of the Vardar river in this part of the watershed are the rivers Pena, Vratnicka and Bistrica. The basic characteristics of these sub watersheds are shown in Table 3.

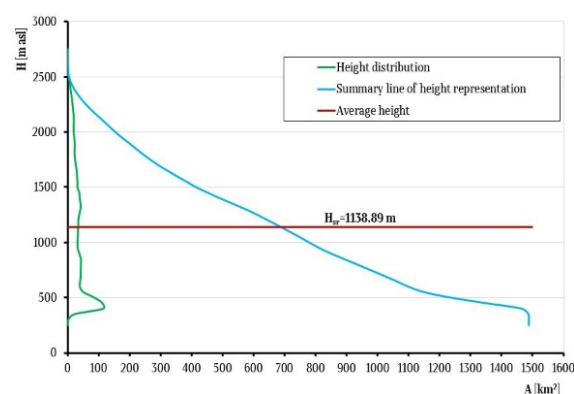


Figure 4. Hypsogram curve of the upper Vardar watershed

Table 3. Geometrical characteristics of the sub watersheds

Profile	$A [km^2]$	$O [km]$	$Ssr [%]$	$Hsr [m \text{ H.B.}]$	$L [km]$
Pena	173.03	93.91	13.49	1681.65	39.35
Vratnicka	30.62	32.70	12.72	1393.26	13.28
Bistrica	39.30	44.35	15.02	1629.66	21.20

## 2.3 GEOLOGICAL AND HYDROGEOLOGICAL CHARACTERISTICS

The section of Vardar River to be regulated represents a part of the Polog valley and belongs to the Vardar tectonic zone. The geological structure of this valley is composed from sedimentary, magmatic and metamorphic rocks dating back to the Paleozoic and Mesozoic as well as Tertiary and Quaternary. The Paleozoic rocks are represented by albite-phyllite mikaschists and green shales, meta-sandy rocks, metaconglomerates, metadiabases, carbonate shales and marbles.



Mesozoic rocks are mainly represented by granites, granodiorites, massive marbleized limestone, diabases, spilites and dunites. Tertiary rocks are developed in the south part of the Polog depression and are represented by pliocene sandy layers with a thickness of 250 m. Quaternary rocks are represented by alluvial sediments, proluvial terraces, fluvio-glacial sediments and disintegrated/moraine materials.

The hydrogeological characteristics of the region can be described by the investigated and recorded aquifers. Phreatic and artesian aquifers are formed in intergranular and unconsolidated sediments. Phreatic aquifers are found in alluvial and proluvial sediments, marbles as well as in the upper Pliocene deposits at the bottom of Shar Mountain. The wells in Tetovo, Gostivar and Miletino belong to these aquifers. Phreatic aquifers belong to the group of aquifers with good yield,  $1 \div 10$  l/s and  $> 10$  l/s. The artesian aquifer is representative for Lower Polog (Dolen Polog) (village Zhilche, village Janchishte, village Jegunovce and village Raotince) and belongs to the upper Pliocene sandy/lacustrine sediments with a thickness of about 40 m. The yield of this aquifer amounts to  $1 \div 10$  l/s.

### 3. HYDROLOGICAL ANALYSIS

Available data for the hydrological study have been found only for the station in Jegunovce (1951-2008) and the station in Radusha (1961-2008). The registered data at both stations are incomplete and they have been completed by correlation links between these two arrays of data. In the series referring to Radusha, there are interruptions in the measured data in the period from 1961 to 1968, while in the series referring to Jegunovce, there are interruptions in the period from 2001 to 2003. In order to determine the characteristic flow values for the Vardar river and define the referent discharge for proportioning the regulated river bed and facilities, hydrological analyses have been conducted for both stations at the downstream/outlet profile of the considered section, v. Jegunovtse and v. Radusha. For analysis of the flood waters, the dates of maximum annual flow have been used, specifically for the period 1951-2008 for Jegunovce and the period 1961-2008 for Radusha. To determine the flow with different return periods, several theoretical distribution functions have been applied: Gumbel, Pearson III type distribution, Log Normal distribution, Log Pearson III type distribution. The graphical presentation of the empirical and theoretical

lines of distribution of the probability of occurrence of the referent flow are shown in Figure 5 for Radusha and in Figure 6 for Jegunovce. The referent flow of the Vardar river at profiles Radusha and Jegunovce determined by the theoretical distribution functions for different probabilities of occurrence is shown in Table 4. For the theoretical distribution functions, adjustment tests have been performed with a 0.05 probability for a test overlap. The testing of the applied theoretical distribution functions has proved the best adjustments for the Gumbel distribution for both profiles.

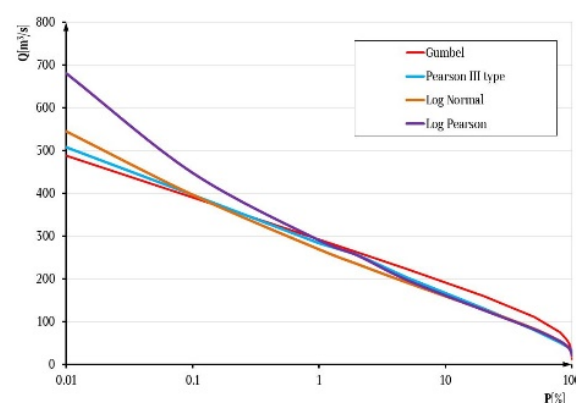


Figure 5. Lines of distribution for Radusha

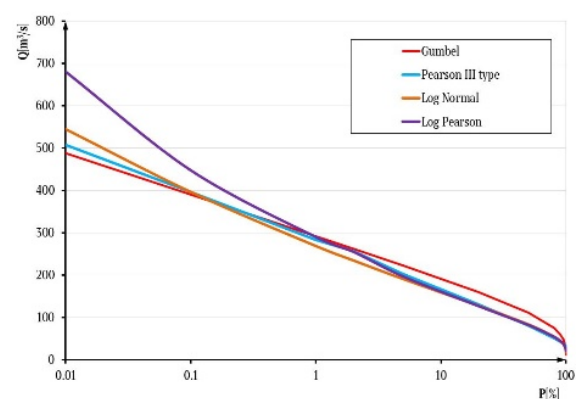


Figure 6. Lines of distribution for Jegunovce

Down to the Radusha profile, the measured flows in the observed period (1951-2008) cover all the upstream tributaries, as well as the released installed quantities from the HPP Raven (in operation for more than 40 years) whose maximum capacity is  $Q=32 \text{ m}^3/\text{s}$ . The defined characteristic flows for the Radusha profile are not much different from those at Jegunovce profile, which is, in fact, a downstream profile or a downstream boundary condition for the analyzed section. According to these statements, the characteristic flows defined for the Radusha profile have been adopted in modeling the flood zones in this part of the Vardar river.

Table 4. Flow determined by the theoretical distribution functions

T [years]	Probability p	p [%]	Radusa				Jegunovce			
			Gumbel	Pearson III type	Log- normal	Log Pearson	Gumbel	Pearson III type	Log- normal	Log Pearson
10000	0.0001	0.01	<b>491.40</b>	498.24	549.45	679.81	<b>487.71</b>	507.18	544.99	680.64
1000	0.0010	0.10	<b>394.13</b>	393.14	405.08	454.96	<b>389.54</b>	395.65	396.44	447.54
100	0.0100	1.00	<b>296.61</b>	285.88	279.08	300.09	<b>291.13</b>	283.04	268.69	289.84
50	0.0200	2.00	<b>267.11</b>	259.61	244.90	265.25	<b>261.36</b>	255.70	234.43	254.81
20	0.0500	5.00	<b>227.73</b>	208.41	200.83	206.75	<b>221.62</b>	202.67	190.58	196.44
10	0.1000	10.00	<b>198.15</b>	174.28	168.73	170.37	<b>191.77</b>	167.14	158.89	167.74
5	0.2000	20.00	<b>165.62</b>	143.72	136.37	135.71	<b>158.94</b>	131.06	127.22	126.58
2	0.5000	50.00	<b>117.74</b>	139.07	90.82	89.52	<b>110.63</b>	80.22	83.23	81.98
1.25	0.8000	80.00	<b>82.12</b>	88.69	60.49	60.20	<b>74.68</b>	50.70	54.45	54.18
1.11	0.9000	90.00	<b>66.99</b>	58.35	48.89	49.37	<b>59.41</b>	41.95	43.60	44.04
1.05	0.9500	95.00	<b>55.88</b>	48.60	41.07	42.28	<b>48.20</b>	37.03	36.35	37.47
1.01	0.9900	99.00	<b>37.71</b>	42.64	29.56	31.63	<b>29.86</b>	32.66	25.78	27.67
1.001	0.9990	99.90	<b>20.56</b>	37.23	20.36	23.32	<b>12.55</b>	31.02	17.47	20.13

## 4. HYDRAULIC ANALYSIS

The hydraulic analysis of the natural riverbed and the solution for the transformation of the flood wave in the investigated Vardar river section, from the bridge in the village of Jegunovce to the bridge in the village of Radusha, have been performed and obtained by using the HEC-RAS software, [16]. The riverbed has a non-prismatic cross-section, almost no straight sections and passes from one meander to another. From field prospecting

and photo documentation, it can be concluded that the river banks are overgrown with dense vegetation and that the riverbed is a recipient of significant amounts of solid and organic waste, which interfere with the flow and cause the river to overflow even in the case of small quantities of water, Figure 7. The bottom of the riverbed is variable, with a reverse slope and expressed erosive deepenings in places, especially in front of bridges. Using the photo documentation from the field, the roughness coefficient of the riverbed has been determined to amount to  $n=(0.030\div0.040) \text{ m}^{-1/3}\text{s}$  and  $n=0.050\div0.100\text{m}^{-1/3}\text{s}$  for the flooded areas.



Figure 7. Photographs from site (field)

### 4.1 ONE-DIMENSIONAL MODEL (1D)

The hydraulic model for simulation of the stationary variable flow in the Vardar riverbed at the analyzed section, in addition to the information on the geometric characteristics of the riverbed, has been defined by the boundary conditions of the flow, upstream and downstream, respectively. For that purpose, the riverbed of the Vardar river has been

modeled from the bridge in the village of Jegunovce to the bridge in the village of Tudence, with a total length of 8504.41 km and a total of 80 cross-sections, Figure 8. The cross-sections have been positioned at different distances from each other, having several different lengths. The analyzed section of the Vardar river starts at chainage km 0+000.00 near the bridge in the village of Jegunovce and extends to chainage km 8+504.41 to a profile at a distance of 500 m

upstream the Tudence bridge. Assigned for the boundaries of the modeled section have been the riverbed slope in the most upstream profile at chainage km 8+504.41,  $S_o = 1.5\text{‰}$  and in the lowest downstream profile at chainage km 0+000.00,  $S_o = 1.47\text{‰}$ , assuming that the flow in these profiles is even and gradually variable. The hydraulic analysis has been performed for 6 valid flows, namely  $Q=24.2 \text{ m}^3/\text{s}$  (average multi-year flow),  $Q=46.1 \text{ m}^3/\text{s}$  (average multi-year flow determined by the maximum monthly flows),  $Q=62 \text{ m}^3/\text{s}$  (critical flow according to UHMR),  $Q=102 \text{ m}^3/\text{s}$  (average multi-year flow determined by the maximum yearly flows),  $Q=227 \text{ m}^3/\text{s}$  ( $Q_{0.05}$ ) and  $Q=267 \text{ m}^3/\text{s}$  ( $Q_{0.02}$ ). In order to determine the impact of the bridges on the propagation of the flood wave in the riverbed and the shape of the water surface, the bridge structures have been modeled with their basic characteristics: type of structure, number of openings, number of piers, width of piers, width of openings, elevation of the

superstructure, elevation of the substructure and angle of the bridge axis in relation to the riverbed, Table 5.

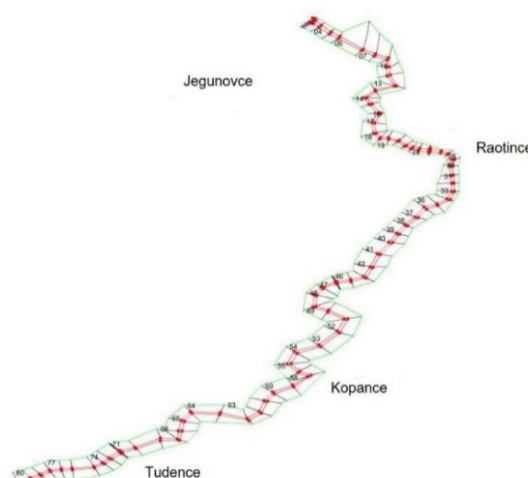


Figure 8. Situation with cross sections of 1D modelling

Table 5. Basic characteristics of the bridges (Source: [17])

Bridge	Type	Stationing [km]	Number of openings	Number of piers	Width of openings [m]	Elev. of upper constr. [m asl]	Elev. of lower constr. [m asl]	Axis
Jegunovce	steel	0+030.39	1	/	38	385.74	384.01	/
Raotince	concrete	2+248.00	3	2	3/13/7.63	386.37	385.39	126
Kopance	concrete	4+262.00	2	3	8.24/7.98	388.67	388.07	65
Tudence	concrete	7+707.00	3	2	6.6/13.5/6	393.43	392.56	66

## 4.2 COMBINATION OF ONE AND TWO-DIMENSIONAL MODEL (1D/2D)

In the combined model of 1D and 2D, the riverbed is considered as one-dimensional element, while the inundations or flood zones are considered as two-dimensional. This means that the flow in the riverbed is a stationary variable flow, while in the inundations, there is a non-stationary flow. For that purpose, the riverbed has been modeled with the characteristic cross-sections and their characteristics, while a georeferenced topographic map has been elaborated for the inundations based on the Photogrammetric Map of Macedonia by use of the ArcMap software, [18]. In order to consider the flow in the inundations and the bank zones as two-dimensional, a 2D network has been generated for the left side of the riverbed with a total of 2407 cells sized 50x50 m and for the right side of the riverbed with a total of 2111 cells sized 50x50 m.



Figure 9. Calculation zone of 1D/2D hydraulic model of the river Vardar



The width of the net depends on the geometry of the terrain and it is usually plotted up to the assumed flood area. The riverbed and these two-dimensional flow zones are interconnected by lateral structures. The lateral structures are positioned along the entire length of the riverbed, starting from the river banks (left and right).

Assigned at the boundaries of the modeled section have been the slope of the river bottom in the most upstream profile at chainage km 8+504.41,  $S_0 = 1.5\text{‰}$  and in the lowest downstream profile at chainage km 0+000.00,  $S_0 = 1.47\text{‰}$ . The roughness coefficient according to Manning for the riverbed is  $n=0.030 \text{ m}^{-1/3}\text{s}$ , while for the two-dimensional surface, it is  $n=0.060 \text{ m}^{-1/3}\text{s}$ . Figure 9 shows the layout of the two-dimensional computational networks and side structures in the hydraulic model.

### 4.3 TWO-DIMENSIONAL MODEL (2D)

In the two-dimensional model of analysis of transformation of the flood wave in the Vardar river, from the bridge in the village of Jegunovce to the bridge in the village of Tudence, the entire analyzed section, the river bed, the inundations and the bank zones are considered as two-dimensional. The flow in this model is non stationary. For that purpose, a georeferenced topographic map has been elaborated for the analyzed section of the Vardar river and a two-dimensional calculation network (area) has been generated for the riverbed, the inundations and the bank zones with a total of 38663 cells of a different size. For better results of the analysis of transformation of the flood wave in the model, the size of the cells in the 2D surface have been variable as follows: in the mid zone of the riverbed, the cells have been sized 2x4 m, in the heel zone of the river bed, the cell size has been 3x5 m, in the bank zone, the cell size has been 5x10 m, in the zone of the inundations, the cell size has been 10x30 m, at a distance of 150 m from the riverbed, the cells have been sized 30x50 m and to the end of the surface, the cells have been sized 100x100 m, Figure 10.

Due to variation of the roughness coefficients in different parts of the surface, 3 zones of variable values have been established, or more precisely, a zone in the riverbed with a roughness coefficient according to Manning of  $n=0.030 \text{ m}^{-1/3}\text{s}$ , an inundation zone with a roughness coefficient of  $n=0.035 \text{ m}^{-1/3}\text{s}$  and bank zones with a roughness coefficient of  $n=0.060 \text{ m}^{-1/3}\text{s}$ .

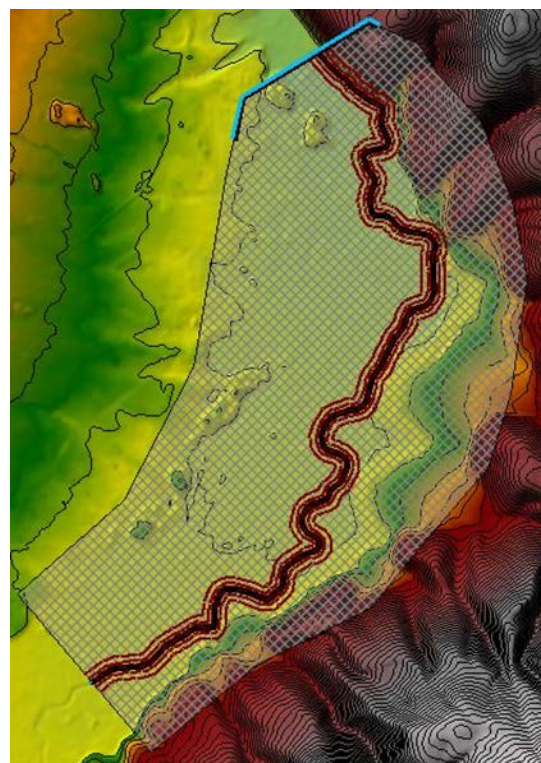


Figure 10. Calculation zone of 2D hydraulic model of the river Vardar

At the boundaries of the modeled section, boundary conditions have been assigned by means of a BC Line (Boundary condition line). In front of the very entry into the surface (according to the river flow), at the village of Tudence, a boundary condition for the beginning of the flow, namely, a flow hydrograph has been assigned, whereas, at the end of the surface, at v. Jegunovce, a boundary condition for the flow end in the form of a slope at normal depth (energy line slope) has been assigned to amount to  $S=1.5 \text{‰}$ .

The inlet flow hydrograph has been generated by means of flows defined during the hydrological analysis. To determine the inflow and outflow time of the hydrograph, the flood wave of Vardar river registered by UHMR at Jegunovce profile for the period 06.05.2005 to 10.05.2005 has been used. The inflow time of the hydrograph has been calculated to amount to  $T_b=30 \text{ hrs}$ , while the outflow time has been calculated to amount to  $T_r=60 \text{ hrs}$ . The construction of the curvilinear hydrograph has been based on the Gauss distribution curve. The established curvilinear hydrograph for the profile near the village of Jegunovce is shown in Figure 11.



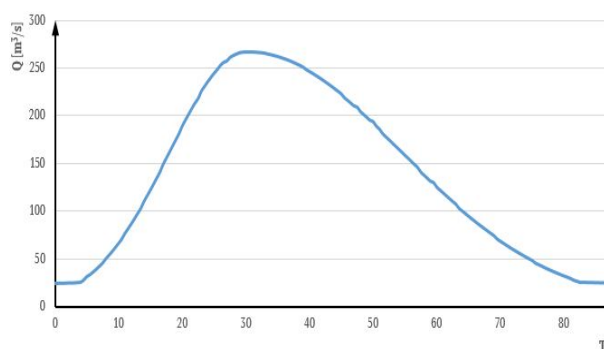


Figure 11. Flow hydrograph for the profile at v.Jegunovce

## 5. ANALYSIS OF RESULTS

The hydraulic analysis conducted by use of the one-dimensional model has shown that, for the flows of  $Q=24.2 \text{ m}^3/\text{s}$  and  $Q=46.1 \text{ m}^3/\text{s}$ , there will be no overflow in any part of the analyzed river section. For flows close to the critical  $Q=62 \text{ m}^3/\text{s}$ , the first overflows occur as presented in Table 6. The same table contains a description of the location of the cross-sections with chainage and lateral (left/right) overflow for the registered critical flow  $Q=62 \text{ m}^3/\text{s}$ .

Table 6. Critical cross sections of overflow

Profile	Stationing [km]	Overflow		Profile	Stationing [km]	Overflow	
		left	right			left	right
5	0+213.92	✓		23	2+102.01		✓
6	0+288.49	✓		28	2+378.25	✓	✓
8	0+610.81	✓		29	2+447.72		✓
9	0+711.52	✓		32	2+733.78	✓	
10	0+819.91	✓		35	3+034.39	✓	
11	0+910.90	✓		36	3+125.80	✓	
12	1+050.71	✓		37	3+251.29	✓	
13	1+205.63	✓	✓	42	3+919.02	✓	✓
14	1+331.20		✓	52	5+035.67		✓
15	1+413.10		✓	62	6+512.07	✓	
16	1+536.07	✓		69	7+586.88	✓	
17	1+652.77	✓	✓	72	7+806.71	✓	
18	1+780.17	✓	✓	73	7+878.63	✓	
19	1+854.71	✓	✓	74	7+956.86	✓	
20	1+913.68	✓	✓	75	8+108.79	✓	
21	1+992.00	✓	✓	76	8+198.70	✓	
22	2+065.49		✓	77	8+265.40		✓

From the conducted hydraulic analysis, it can be concluded that the riverbed of the Vardar river in the analyzed region, from the village Tudence to the village Jegunovce, can safely transform flows up to  $Q=62 \text{ m}^3/\text{s}$ . Larger flows cause the river to overflow, with the first flooded zones appearing upstream from the village Raotince. With the increase of the water level, the overflow intensifies and the flooded zones become bigger, Figure 12. The flow regime for all characteristic flows is subcritical and the Froude numbers are less than the critical value,  $Fr < 1$ . Small and medium flows pass through the bridge openings without any problems. However, the observed deepening of the bottom in the area of the bridges, indicates the

presence of erosion of the bridge piers even at these small flows. The position of the bridges and the layout of the bridge piers are hydraulically unfavorable and cause flow slow down, raising the level in the riverbed upstream the bridges. The bridges in the analyzed region generally sustain flows of up to  $Q=100 \text{ m}^3/\text{s}$  without any overflow. The bridge near the village of Tudence safely sustains a flow of  $Q=102 \text{ m}^3/\text{s}$ . At  $Q=228 \text{ m}^3/\text{s}$ , no overflow is registered, but the flow is under pressure, endangering the bridge. The bridge in the village of Kopance has the smallest capacity, meaning that the flow is under pressure at  $Q=102 \text{ m}^3/\text{s}$ , while in the case of bigger flows, there is an overflow outside the riverbed. The

bridge in the village of Raotince safely sustains a flow of  $Q=102 \text{ m}^3/\text{s}$ , while there are signs of flow under pressure at around  $Q=130 \text{ m}^3/\text{s}$ . At the maximum flows with a return period of 20 and 50 years,  $Q=228 \text{ m}^3/\text{s}$  and  $Q=267 \text{ m}^3/\text{s}$ , there is an overflow in the riverbed in inhabited places. The bridge near the village of Jegunovce can be said to be the safest compared to the other bridges. The bridge has a sufficient capacity to sustain all of the analyzed flows. At a flow of  $Q=62 \text{ m}^3/\text{s}$ , the velocities in the riverbed are in the range of  $V=0.83 \text{ m/s}$  to  $V=2.27 \text{ m/s}$ . The flow velocities in the riverbed at a flow of  $Q=102 \text{ m}^3/\text{s}$  are in the range of  $V=1.08 \text{ m/s}$  to  $V=2.66 \text{ m/s}$ . At a flow of  $Q=228 \text{ m}^3/\text{s}$ , the velocities in the riverbed are in the range of  $V=1.17 \text{ m/s}$  to  $V=3.36 \text{ m/s}$ . In the analysis done for the maximum flow of  $Q=267 \text{ m}^3/\text{s}$ , the biggest values for the flow velocity occur and they are in the range of  $V=1.21 \text{ m/s}$  to  $V=3.51 \text{ m/s}$ .

From the analysis of flood wave transformation by use of the combined model of one- and two-dimensional flow, it has been concluded that, at small flows of  $Q=24.2 \text{ m}^3/\text{s}$  and  $Q=46.1 \text{ m}^3/\text{s}$ , there is no overflow in the riverbed. The first overflows occur at a flow of  $Q=62 \text{ m}^3/\text{s}$ , in the left inundation, near the village of Raotince, Figure 13-a. From the conducted hydraulic analysis by use of the combined model, it can be concluded that, at a flow of  $Q=102 \text{ m}^3/\text{s}$ , there are overflows in the following cross-sections of the analyzed river: km 0+950.00 to km 2+120.00, km 2+350.00 to km 3+250.00, km 3+900.00 to km 4+200.00, km 4+500.00 to km 4+700.00, km 5+000.00 to km 5+250.00, km 5+570.00 to km 6+500.00, km 6+800.00 to km 7+020.00 and from km 8+100.00 to km 8+427.61, Figure 13-b. The flooded area during this flow covers about 35 ha. At a flow of  $Q=228 \text{ m}^3/\text{s}$ , an overflow occurs along the entire length of Vardar river, from the village of Tudence to the village of Jegunovce, Figure 13-c, the flooded agricultural area covering 510 ha, while at a flow of  $Q=267 \text{ m}^3/\text{s}$ , the flooded area increases to about 600 ha, Figure 13-d. At a flow of  $Q=62 \text{ m}^3/\text{s}$ , the flow velocities in the riverbed are in the range of  $V=0.88 \text{ m/s}$  to  $V=4.21 \text{ m/s}$ , while the flow velocities in the flooded areas are in the range of  $V=0.03 \text{ m/s}$  to  $V=0.83 \text{ m/s}$ . The maximum amount of flow that occurs in the flooded areas is  $Q=4.56 \text{ m}^3/\text{s}$ . Flow velocities in the riverbed at a flow of  $Q=102 \text{ m}^3/\text{s}$  are in the range of  $V=1.03 \text{ m/s}$  to  $V=4.71 \text{ m/s}$ , while the flow velocities in the flooded areas are in the range of  $V=0.10 \text{ m/s}$  to  $V=0.91 \text{ m/s}$ . The maximum amount of flow that occurs in the flooded areas is  $Q=37.83 \text{ m}^3/\text{s}$ . At a flow of  $Q=228 \text{ m}^3/\text{s}$ , the flow velocities in the

riverbed are in the range of  $V=1.24 \text{ m/s}$  to  $V=5.73 \text{ m/s}$ , while the flow velocities in the flooded areas are in the range of  $V=0.28 \text{ m/s}$  to  $V=1.00 \text{ m/s}$ . The maximum amount of flow that occurs in the flooded areas is  $Q=121.19 \text{ m}^3/\text{s}$ . In the analysis for the maximum flow of  $Q=267 \text{ m}^3/\text{s}$ , the biggest flow velocities occur and they are in the range of  $V=1.26 \text{ m/s}$  to  $V=5.99 \text{ m/s}$  for the riverbed and in the range of  $V=0.14 \text{ m/s}$  to  $V=1.00 \text{ m/s}$  for the flooded areas. The maximum amount of overflow is  $Q=156.25 \text{ m}^3/\text{s}$ .

As in the case of the previous two models, the conclusion from the analysis done by use of the two-dimensional model is that, at small flows of  $Q=24.2 \text{ m}^3/\text{s}$  and  $Q=46.1 \text{ m}^3/\text{s}$ , there is no overflow in the riverbed. The first overflow occurs at a flow of  $Q=62 \text{ m}^3/\text{s}$  along the entire river, Figure 14. From the hydraulic analysis conducted by use of the two-dimensional model, it is concluded that, at a flow of  $Q=62 \text{ m}^3/\text{s}$ , the flow velocities in the riverbed are in the range of  $V=0.75 \text{ m/s}$  to  $V=3.92 \text{ m/s}$ , while the flow velocities in the flooded areas are in the range of  $V=0.03 \text{ m/s}$  to  $V=0.76 \text{ m/s}$ , Figure 16-a. The maximum depth in the flooded areas is  $H=0.62 \text{ m}$ , Figure 15-a. The flow velocities at a flow of  $Q=102 \text{ m}^3/\text{s}$  are in the range from  $V=0.91 \text{ m/s}$  to  $V=4.22 \text{ m/s}$  in the riverbed and in the range of  $V=0.08 \text{ m/s}$  to  $V=0.83 \text{ m/s}$  in the flooded areas, Figure 16-b. The maximum depth in the flooded areas is  $H=0.75 \text{ m}$ , Figure 15-b. At a flow of  $Q=228 \text{ m}^3/\text{s}$ , the flow velocities in the riverbed are in the range of  $V=1.04 \text{ m/s}$  to  $V=5.18 \text{ m/s}$ , while the flow velocities in the flooded areas are in the range of  $V=0.19 \text{ m/s}$  to  $V=0.95 \text{ m/s}$ , Figure 16-c. The maximum depth in the flooded areas is  $H=1.27 \text{ m}$ , Figure 15-c. In the analysis for the maximum flow of  $Q=267 \text{ m}^3/\text{s}$ , the biggest flow velocities occur and they are in the range of  $V=1.08 \text{ m/s}$  to  $V=5.64 \text{ m/s}$  in the riverbed and in the range of  $V=0.20 \text{ m/s}$  to  $V=1.01 \text{ m/s}$  in the flooded areas, Figure 16-d. The maximum depth in the flooded areas is  $H=1.48 \text{ m}$ , Figure 15-d.

## 6. CONCLUSION

From the hydraulic analyses carried out by use of all three models, it is concluded that the riverbed of the Vardar river in the considered section has a very low transportation capacity and that there are flood zones along the entire length of the river. The most critical points in this section are located near the village of Raotince, the village of Kopance and the village of Tudence, where flood zones occur in

agricultural lands and inhabited places under a slight increase of flood waters.

The research that has been done so far points out the importance of having high quality input data such as high quality field documentation, high quality hydrological and hydraulic analyses, available public data for the conducting of high quality analyses of flood wave propagation and determination of flood zones. The time frame for calculations and analysis of hydraulic parameters is significantly shortened by using the HEC-RAS software. The software enables fast, accurate and precise modeling of the riverbed with all the

accompanying facilities, which is extremely important in determining the flood zones and their prevention. The ability to create different types of models such as one-dimensional, two-dimensional or a combination of both is a step forward in the analysis of flood zones.

The high quality results from the hydraulic models can be used as input parameters in preparation of maps of critical zones in floodplains. These maps can be used for analysis of flood zones, flood disaster prevention preparedness and management of the affected areas in the event of a major flood wave.

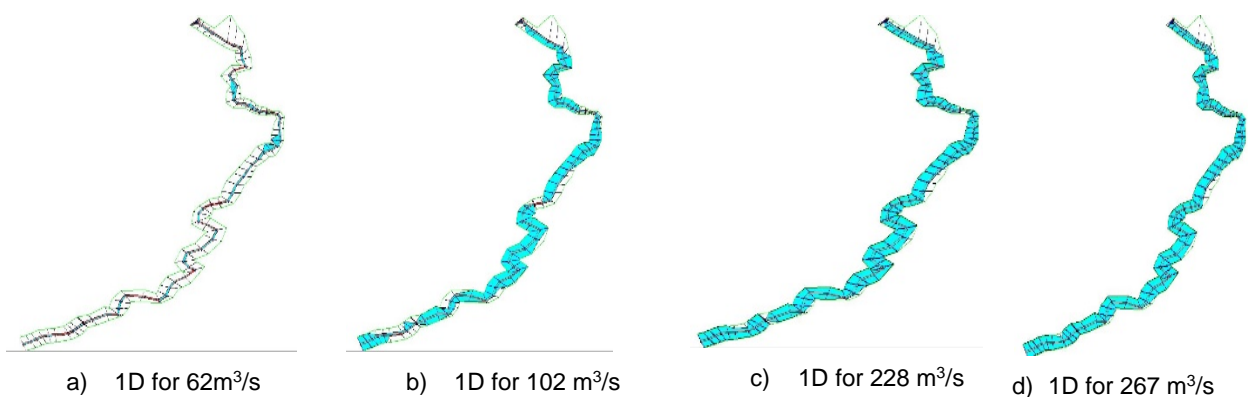


Figure 12. Flood area of 1D model

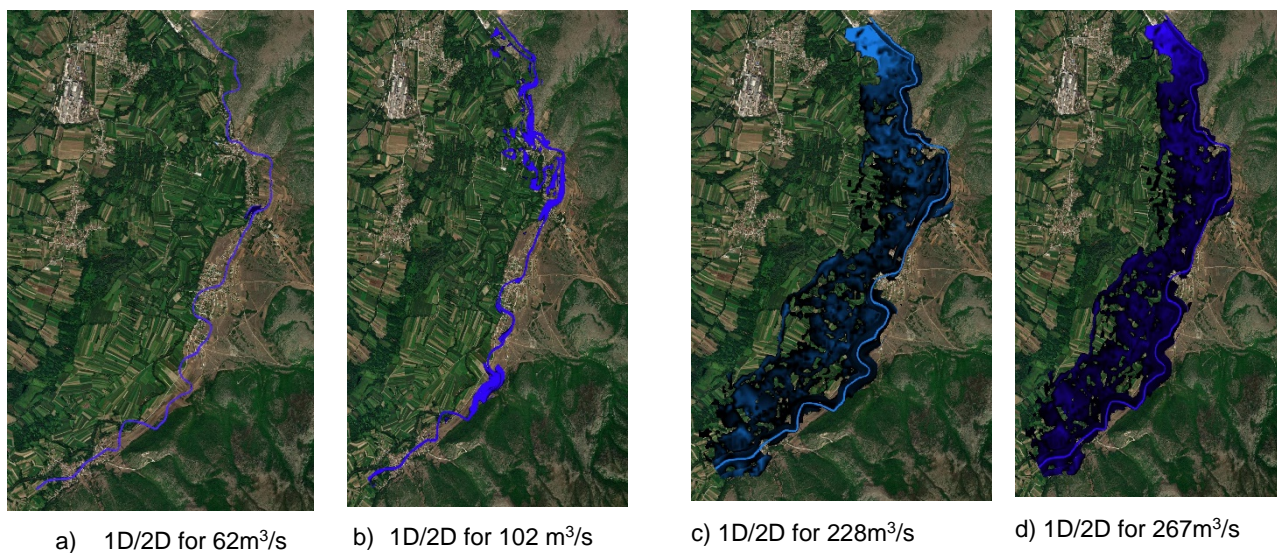


Figure 13. Flood area of 1D/2D model



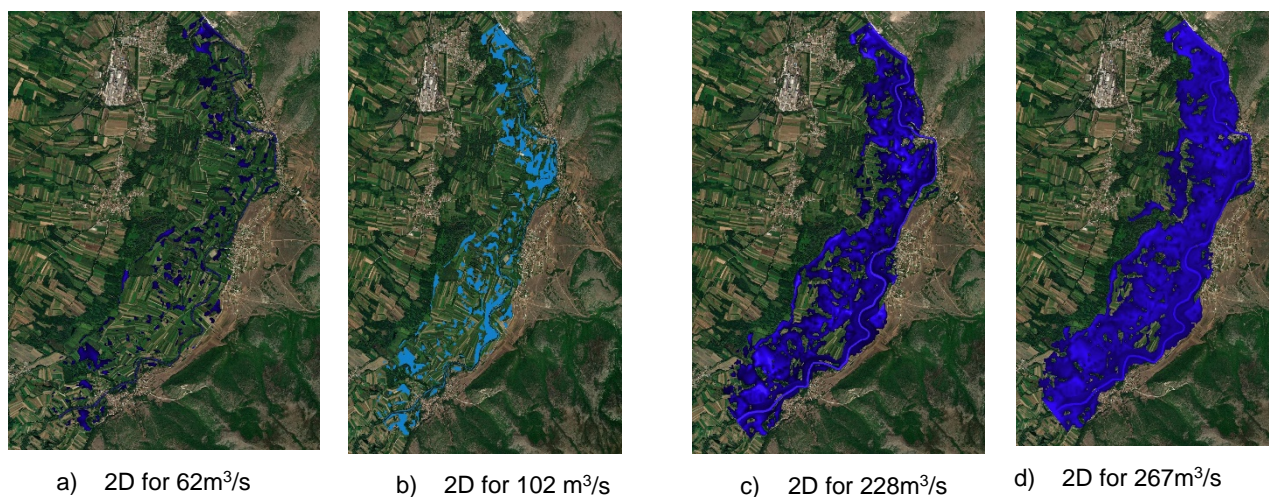


Figure 14. Flood area of 2D model

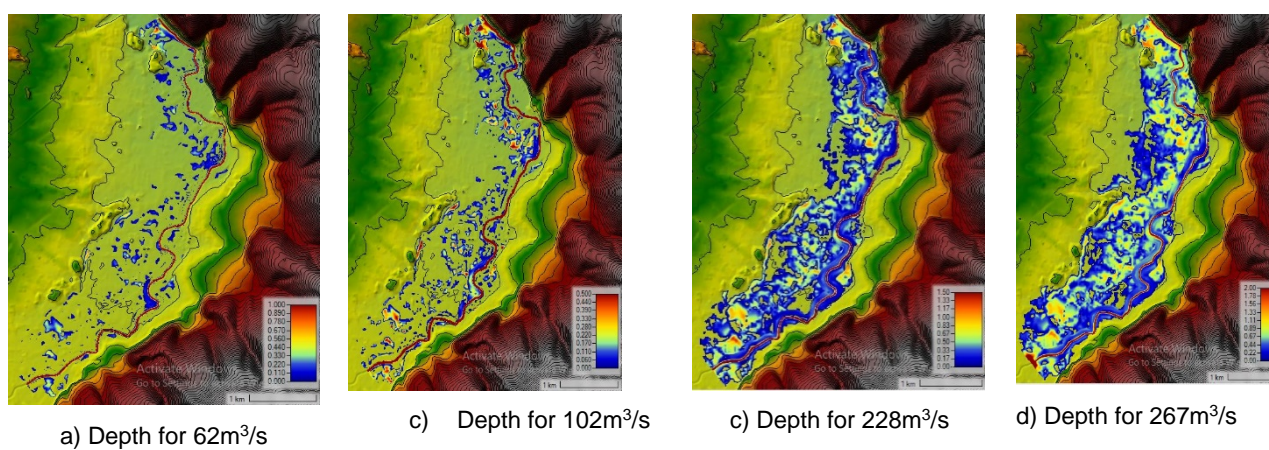


Figure 15. Water depth of 2D model

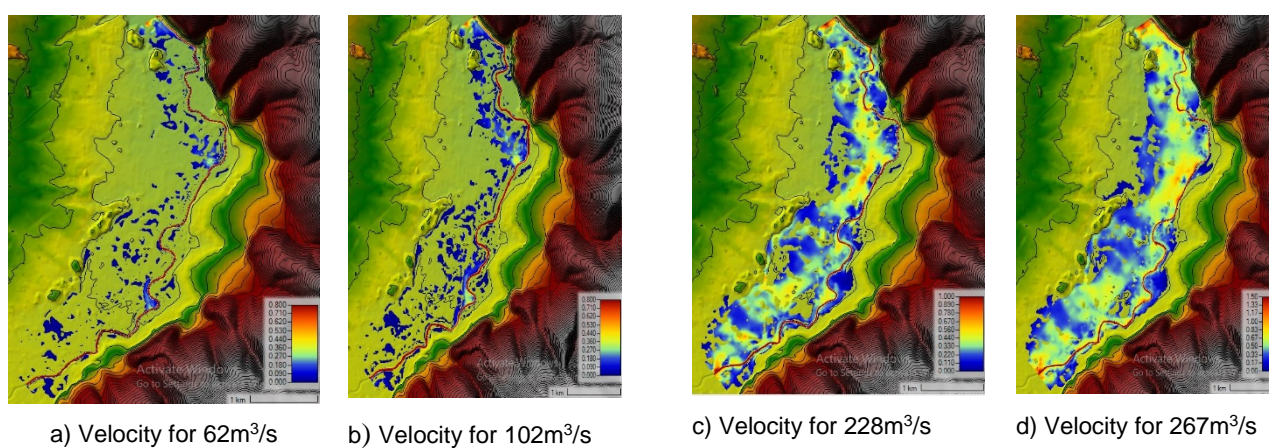


Figure 16. Water velocity of 2D model

## REFERENCES

- [1] E. Morin, Y Jabocy, S Navon, and E Bet-Halachmi, "Towards flash-flood prediction in the dry Dead Sea region utilizing radar rainfall information," *Advances in Water Resources*, vol.32, pp. 1066-1076, 2009.
- [2] C. C. Abon, C P David, and N B Pellejera, "Reconstructing the Tropical Storm Ketsana flood event in Marikina River, Philippines," *Hydrology and Earth System Sciences*, vol. 15, no. 4, pp. 1283-1289, 2011.
- [3] Ali, A. A., Al-Ansari, N. A., and Knutsson, S., (2012): Morphology of Tigris River within Baghdad City, *Hydrol. Earth Syst. Sci.*, 16, 3783–3790, <https://doi.org/10.5194/hess-16-3783-2012>.
- [4] Santillan J.R., Dr. Paringit E.C., (2013): Modeling of Flash-flood Events using Integrated GIS and Hydrological Simulations. SMTFCMMS, Philippines.
- [5] Hong Q. N., et al., (2015): „Flash flood prediction by coupling KINEROS2 and HEC-RAS models for tropical regions of Northern Vietnam". *Hydrology* 2015, 2, 242-265; doi:10.3390/hydrology2040242.
- [6] Thaileng T.; et al., (2016): „Application of HEC-RAS for a flood study of a river reach in Cambodia". *Vietnam*, pp. 16-20.
- [7] Vassiliki T. G. B., et al., (2017): „Hydrological impacts of urban developments: modelling and decision-making concepts". *Theoretical and Empirical Researces in Urban Management*, v 12 i 4.
- [8] Romali, N., Yusop, Z. and Ismail, A., 2018. Application of HEC-RAS and arcGIS for floodplain mapping in Segamat town, Malaysia. *International Journal of GEOMATE*, 15(47).
- [9] Ben Khalfallah, C. and Saidi, S., (2018). Spatiotemporal floodplain mapping and prediction using HEC-RAS - GIS tools: Case of the Mejerda river, Tunisia. *Journal of African Earth Sciences*, 142, pp.44-51.
- [10] Dasallas, L.; Kim, Y.; An, H., (2019): Case Study of HEC-RAS 1D–2D Coupling Simulation: 2002 Baeksan Flood Event in Korea., 11, 2048.
- [11] Diedhiou, R., et al., (2020). Calibration of HEC-RAS Model for One Dimensional Steady Flow Analysis—A Case of Senegal River Estuary Downstream Diama Dam. *Open Journal of Modern Hydrology*, 10(03), pp.45-64.
- [12] Huțanu, E.; et al., (2020): Using 1D HEC-RAS Modeling and LiDAR Data to Improve Flood Hazard Maps Accuracy: A Case Study from Jijia Floodplain (NE Romania)., 12, 1624.
- [13] Ilioski B., (2021): "Application of HEC-RAS for analysis of flooding areas", Master thesis, Faculty of Civil Engineering, Skopje, Macedonia.
- [14] Grassland, Soil & Water Research Laboratory, Temple, Texas (2012): Soil and Water Assessment Tool User's Manual.
- [15] Copernicus Land Monitoring Service (CLMS) & European Environmental Agency (EEA), (2012): Corine Land Cover.
- [16] US Army Corps of Engineers, Hydrologic Engineering Center, (February 2016): Hydraulic Reference Manual Version 5.0.
- [17] Faculty of Civil Engineering, (2016): „Regulation of the river Vardar in the Polog region ". Skopje, Macedonia.
- [18] Tiffany Schanatre, MGEO (2014): ESRI ArcMap 10.1 Manual For Hydrography & Survey Use. [www.Geo-Tiff.com](http://www.Geo-Tiff.com).